Mechanical Alloying of Binary Fe – M (M = C, Si, Ge, Sn) Systems: Kinetics, Thermodynamics and Mechamism of Atomic Mixing

EUGENE P. YELSUKOV and GENNADY A. DOROFEEV

Physical-Technical Institute, Ural Centre of the Russian Academy of Sciences, Ul. Kirova 132, Izhevsk 426001 (Russia)

E-mail: Yelsukov@fnms.fti.udmurtia.su

Abstract

The processes of mechanical alloying in the Fe – M (M = C, Si, Ge, Sn) systems at the atomic ratios of 68 : 32 and 75 : 25 under identical conditions of mechanical treatment are studied by X-ray diffraction, Mössbauer spectroscopy, magnetic measurements and thermodynamic simulation. General regularities and differences in the mechanisms and kinetics of solid-state reactions are revealed. A microscopic model of mechanical alloying in these systems is suggested.

INTRODUCTION

One of the main points in studying mechanical alloying (MA) is finding out microscopic mechanisms of solid state reactions (SSR), in particular, those of forming supersaturated solid solutions. In other words, what do we imply by the term "deformation atomic mixing"? It is also necessary to answer the question on the driving forces responsible for the supersaturation effects even in the systems with positive enthalpy of mixing and find out the major factors determining the SSR kinetics.

Appropriate model systems for such an investigation are binary powder mixtures of Fe with isoelectron sp-elements (M = C, Si, Ge, Sn). The ratio of the covalent radii R_M/R_{Fe} changes in a wide range (0.66, 0.95, 1.04, 1.21, respectively). The equilibrium diagrams of the Fe – M alloys are characterized by different types: with actual absence of solubility of the M atoms in a-Fe (Fe – C), with low solubility (Fe – Sn) and broad concentration range of solid solutions (Fe – Si, Fe – Ge).

Mechanical alloying in the Fe – M systems has been attracting much attention of many research teams for the last 10–12 years. A detailed analysis of the data published is presented in our papers [1–4] (Fe – Sn), [4, 5] (Fe – Si), [5, 6] (Fe – C) and [7] (Fe – Ge). We have ascertained that detailed comparison of the mechanisms and kinetics of MA in the Fe – M systems on the basis of the earlier published data is not possible for the following reasons:

1. MA was carried out under different conditions: the material of grinding tools, power intensity of milling devices. The latter characteristic has not been presented;

2. There are considerable differences in the results published.

In the present work we have classified the results of investigation in [1–7] of the mechanisms, kinetics and thermodynamics of MA in the Fe – M (M = C, Si, Ge, Sn) systems under identical treatment conditions in a mill with the known power intensity and controlled levels of contamination and heating of the samples studied.

EXPERIMENTAL

For MA, the mixtures of pure Fe (99.99) and pure *sp*-elements (99.99) powders with the

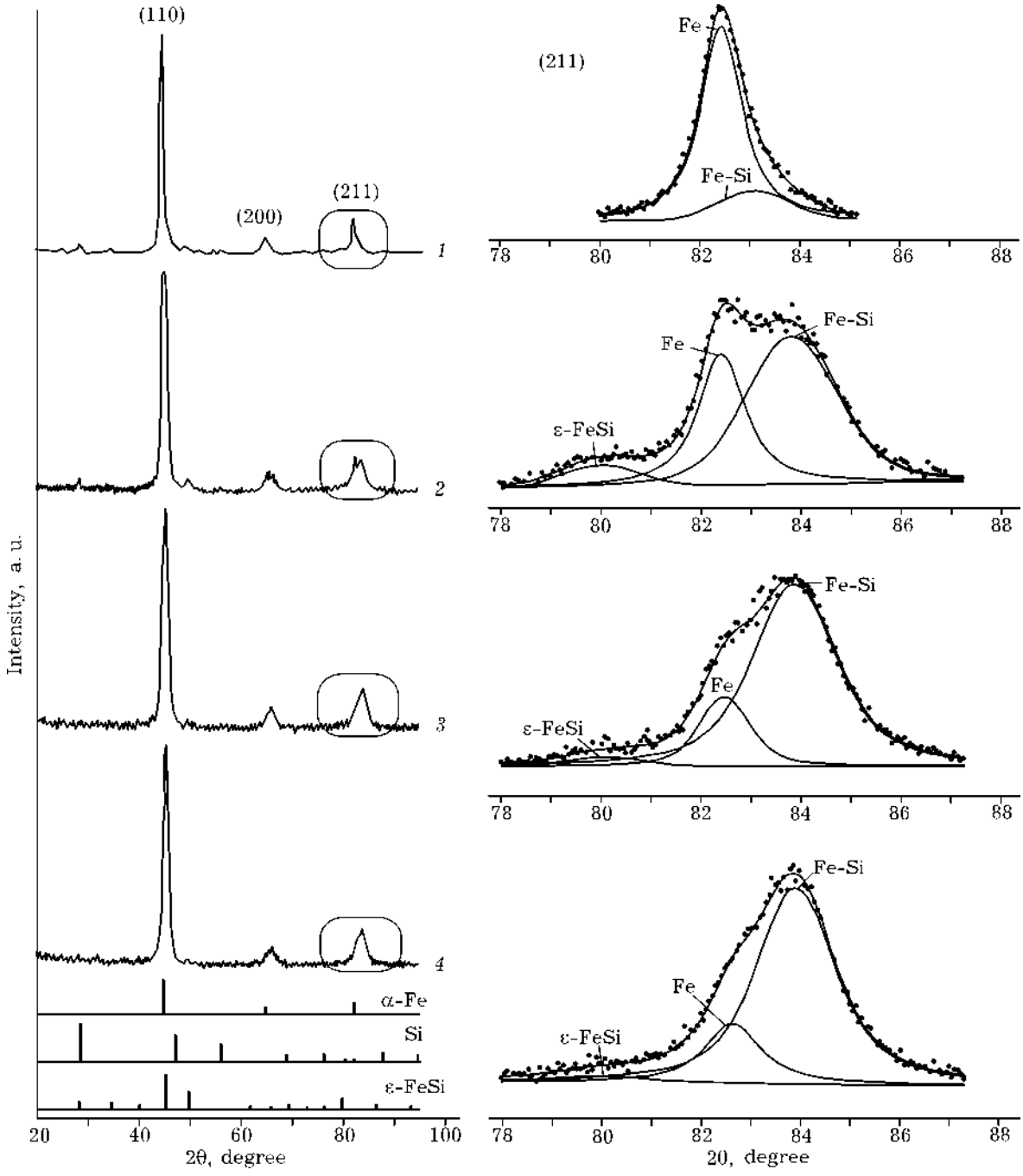

Fig. 1. X-ray diffraction patterns and the results of the decomposition of the *bcc* (211) line for the Fe(68)Si(32) mixture as a function of milling time. t_{mil}, h: 2 (*1*), 8 (*2*), 32 (*3*), and 48 (*4*).

particle size less than 300 mm at atomic ratios of 68 : 32 and 75 : 25 were taken. MA was carried out in an inert atmosphere (Ar) in a planetary ball mill Fritsch P-7 with the power intensity of 2.0 W/g. With air-forced cooling, the heating of the vials, balls and sample did not exceed 60 ℃. The milling tools: vials (volume 45 cm^3) and balls (20, diameter 10 mm) were made of hardened steel containing 1 mass % C and 1.5 mass % Cr. For each given mechanical treatment time, the mass of the loaded sample was m_0 = 10 g. Possible getting of the milling tools material into the sample was monitored by the measurement of the powder mass before and after treatment. For the maximum time of mechanical treatment (t_{mil}), no mass increase of the ground powder (Dm/m_0) for the Fe(68)Sn(32) and Fe(68)Ge(32) systems was

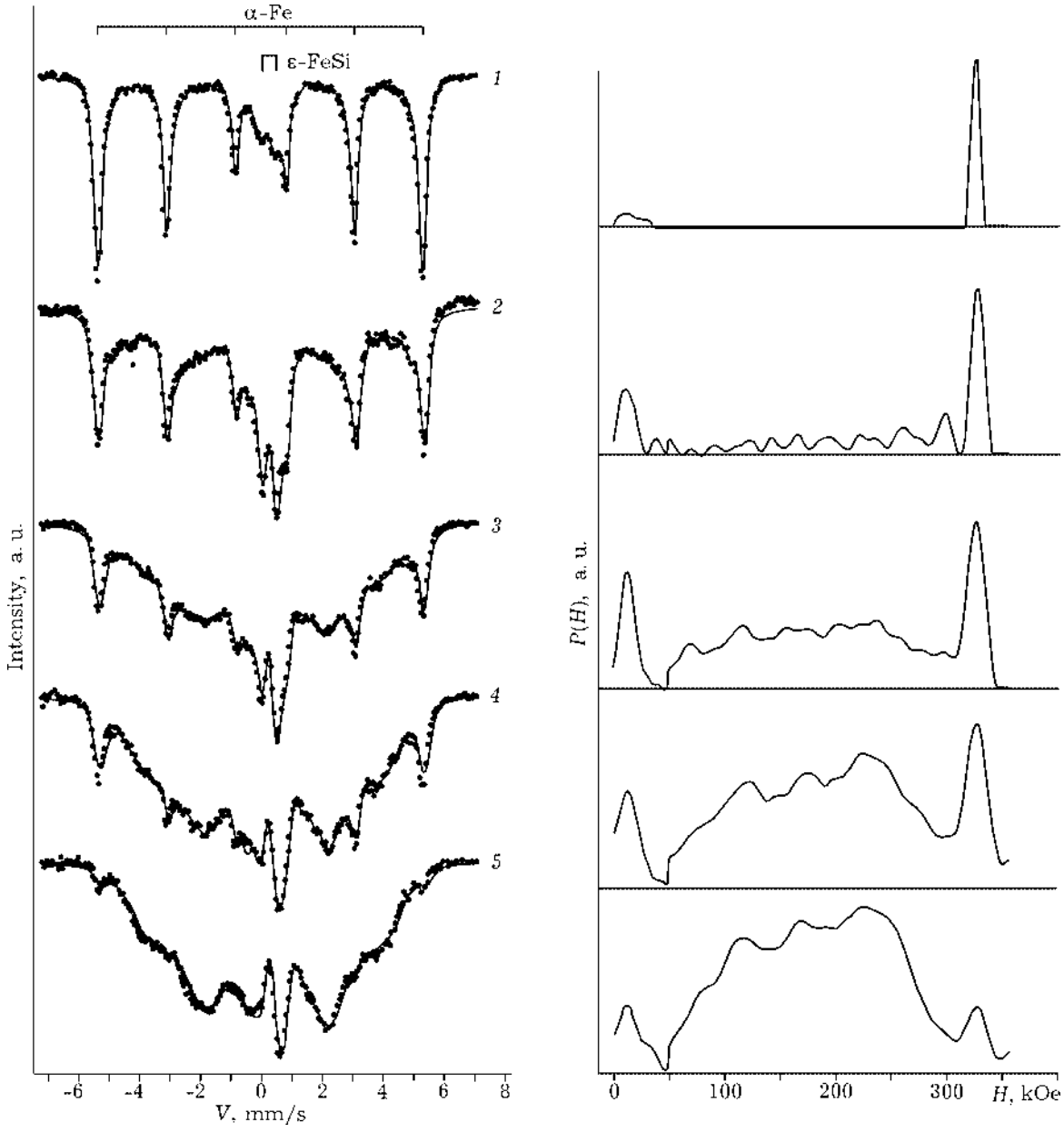

Fig. 2. Mössbauer spectra and $P(H)$ functions for the Fe(68)Si(32) mixture at different milling time. t_{mil}, h: 1 (*1*), 4 (*2*), 8 (*3*), 32 (*4*), and 48 (*5*).

observed. The values Dm/m_0 in case of other systems were as follows: Fe(68)Si(32) – 10 %; Fe(68)C(32) – 10 %, Fe(75)Si(25) – 2 % and Fe(75)C(25) – 1 %. For all the systems $Dm/m_0 = 0$ at $t_{mil} \geq 8$ h.

Mössbauer studies were performed using ^{57}Co in the Cr matrix and ^{119m}Sn in the $CaSnO_3$ matrix sources. X-ray diffraction studies were carried out with monochromatized CuK_a radiation. The temperature of measurements was 300 K. Thermomagnetic measurements were performed in an inert atmosphere (Ar) in the temperature range from 300 to 800 K using an a. c. magnetic susceptibility device. The Miedema's method was applied to estimate the thermodynamic state of phases.

RESULTS AND DISCUSSION

Mechanical alloying in Fe(68)M(32) (M = Si, Ge, Sn) mixtures

Figure 1 shows X-ray diffraction patterns, Fig. 2 – Mössbauer spectra (MS) with corre-

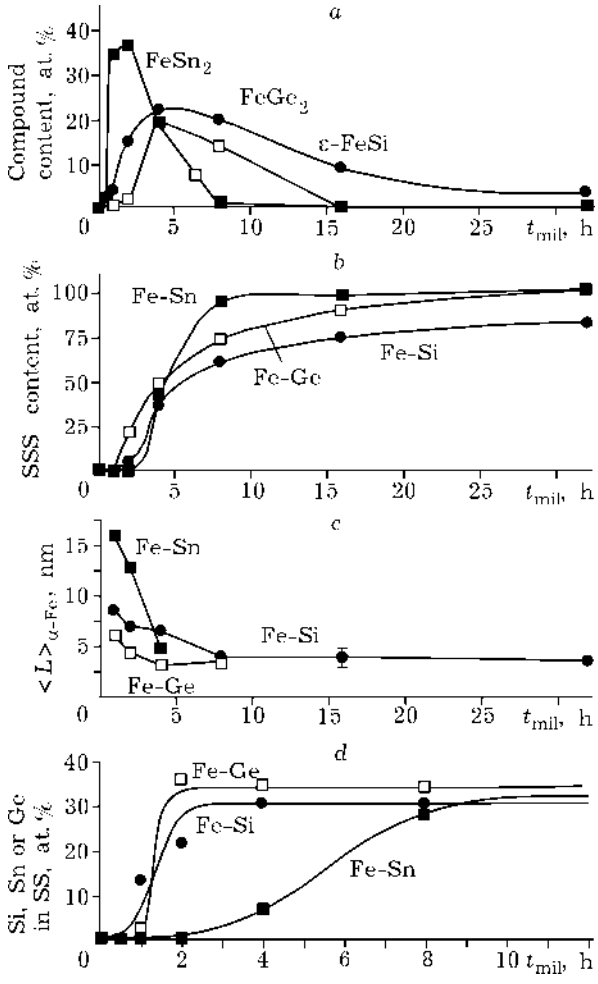

Fig. 3. Time dependences of the amount of intermetallic compounds (*a*), supersaturated solid solutions (*b*), a-Fe grain sizes (*c*) and the *sp*-elements concentration in the solid solution (*d*) during MA in the Fe(68)M(32) (M = Si, Ge, Sn) systems.

sponding distribution functions $P(H)$ obtained at different stages of milling the mixture of a-Fe and b-Si. From the diffraction patterns one can conclude that the *bcc* phase peaks are broadened and alloying begins with the formation of the e-FeSi intermetallic compound of the B20 type, the characteristic peak of which is seen close to $2\theta = 50°$. The presence of the e-FeSi phase is revealed in the MS as a doublet. With the milling time increase in the MS and $P(H)$ functions along with the components from e-FeSi and a-Fe (H = 330 kOe) there appears a component with a broad distribution of hyperfine magnetic fields (HFMF) from 50 to 300 kOe which can be attributed to the a-Fe(Si) supersaturated solid solution (SSS). Simultaneous availability of two bcc phases is distinctly fixed in the shape of (211) line in the diffraction pattern in Fig. 1. The lattice parameter of Si-poor phase did not vary and corresponded to that of a-Fe (0.2866 nm). The parameter of Si-richer *bcc* phase considerably decreased during MA reaching the value of 0.2825 nm at t_{mil} = 4 h and did not change under further treatment. The value obtained agrees well with the bcc lattice parameter of disordered nanocrystalline Fe alloys with 30–31 at. % Si prepared by both MA [8] and mechanical grinding of initially equilibrium alloys [9]. The same Si concentration values in SSS were obtained from the Curie temperature data and average HFMF for broad distribution in $P(H)$ functions.

Thus, MA in the Fe(68)Si(32) system proceeds in two stages. At the first stage, the most stable e-FeSi compound is formed; during the second one – SSS with the Si concentration being approximately equal to the composition of the initial mixture. SSR in the Fe(68)Ge(32) and Fe(68)Sn(32) systems are qualitatively similar to those in the Fe(68)Si(32) system. The difference is that at the first stage the $FeGe_2$ and $FeSn_2$ are formed.

It is of interest to compare the dependences of the phase amount, Si (Ge, Sn) concentrations in SSS and structure parameters for the given systems on the milling time in MA. Figure 3, *a* and *b* collect the time dependences of the compounds and SSS amount; Fig. 3, *c* shows the grain size $\langle L \rangle$ dependences of the unalloyed a-Fe. Their comparison shows that all SSR take place on a-Fe reaching a nanocrystalline state, a smaller grain size being necessary to form SSS than to form an intermetallic compound. For all the systems, an average grain size in SSS of a-Fe(M) is 2–4 nm. The values of microstrains $\langle e^2 \rangle^{1/2}$ are 0.02–0.03 % for a-Fe and 0.2–0.3% for a-Fe(M) SSS.

The type of *sp*-element influences the kinetics. Let us consider two extreme cases: MA in the Fe – Si and Fe – Sn systems. The $FeSn_2$ is formed and disappears fast, meanwhile the rate of the e-Fe – Si formation is slower, and it is present during the whole MA process (see Fig. 3, *a*). As for SSS, it is also formed much faster in the Fe – Sn system than in the Fe – Si

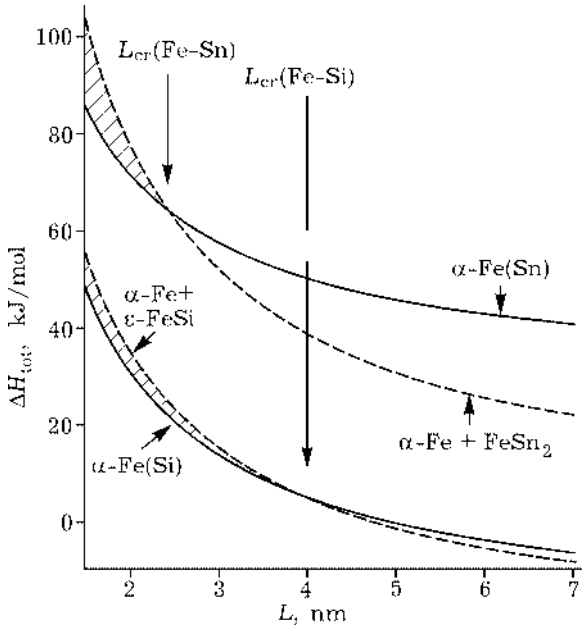

Fig. 4. Total enthalpies of formation of solid solution and mixture of a-Fe + intermetallic compound as a function of grain size.

one (see Fig. 3, *b*). However, a different situation takes place in the saturation of solid solutions (see Fig. 3, *d*). In the Fe – Si system the maximum Si concentration sets in actually simultaneously with the formation of the solid solution, meanwhile in the Fe – Sn system the solid solution is saturated with Sn gradually.

Obviously, the similarities and essential differences observed in the behaviour of the systems in MA are connected with their thermodynamic and kinetic peculiarities. The appearance of compounds at the first stage of MA is due to decrease of free energy because of negative enthalpy of their formation. Figure 4 shows the results of the calculation of the second stage of MA taking into account the interfacial energy and grain boundary segregation of *sp*-elements [3] as dependences of the stored enthalpy of the solid solution formation as well as the a-Fe phase + intermetallic phase mixture for the Fe – Si and Fe – Sn systems on the crystallite sizes. On reaching the grain size of several nanometers (L_{cr}), the SSS formation from the phase mixture becomes energetically favourable. The shaded area at $L < L_{cr}$ characterizes this energy gain which is higher in the Fe – Sn system than in the Fe – Si system. If we consider the $L_{cr} - L = 1$ nm interval, we will obtain the gain of 20.4 kJ/mol for the Fe – Sn system, and 1.3 kJ/mol for the Fe – Si system. In other words, the low rate of transformation in the Fe – Si system in comparison with the Fe – Sn system is accounted for by a different energy driving force of the process.

Mechanical alloying in Fe(75)M(25) (M = Si, C) and Fe(68)C(32) mixtures

The mechanical alloying of the Fe(75)Si(25) mixture is characterized by the same sequence of SSR as in the Fe(68)Si(32) one. Thus, the main focus in this section is on MA of the Fe(75)C(25) mixture. X-ray diffraction patterns, Mössbauer spectra with corresponding $P(H)$ functions and temperature dependences of magnetic susceptibility c(T) of the Fe(75)C(25) samples after MA are presented in Figs. 5, 6 and 7, respectively. Up to $t_{mil} = 2$ h, the diffraction patterns exhibited only *bcc* a-Fe peaks with an unusually large width at the foot of the (110) peak reminding of the halo contribution from the amorphous structure (see Fig. 5). In the Mössbauer spectra at $t_{mil} \leq 2$ h, the main contribution is also made by the component from pure a-Fe (see Fig. 6, *a*). Nevertheless, judging by both the location of the spectrum

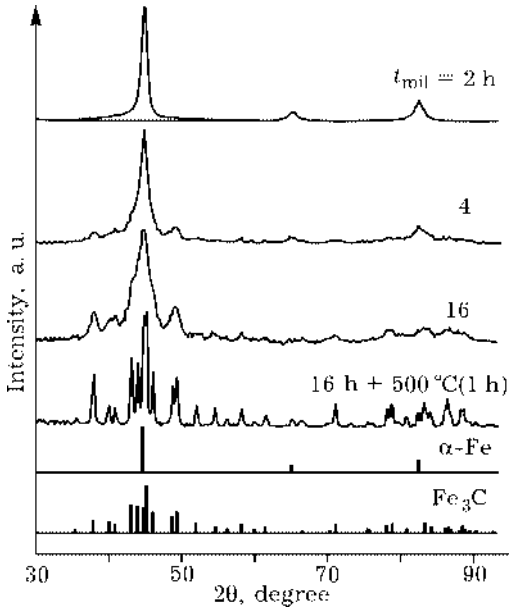

Fig. 5. X-ray diffraction patterns of MA products in Fe(75)C(25) system.

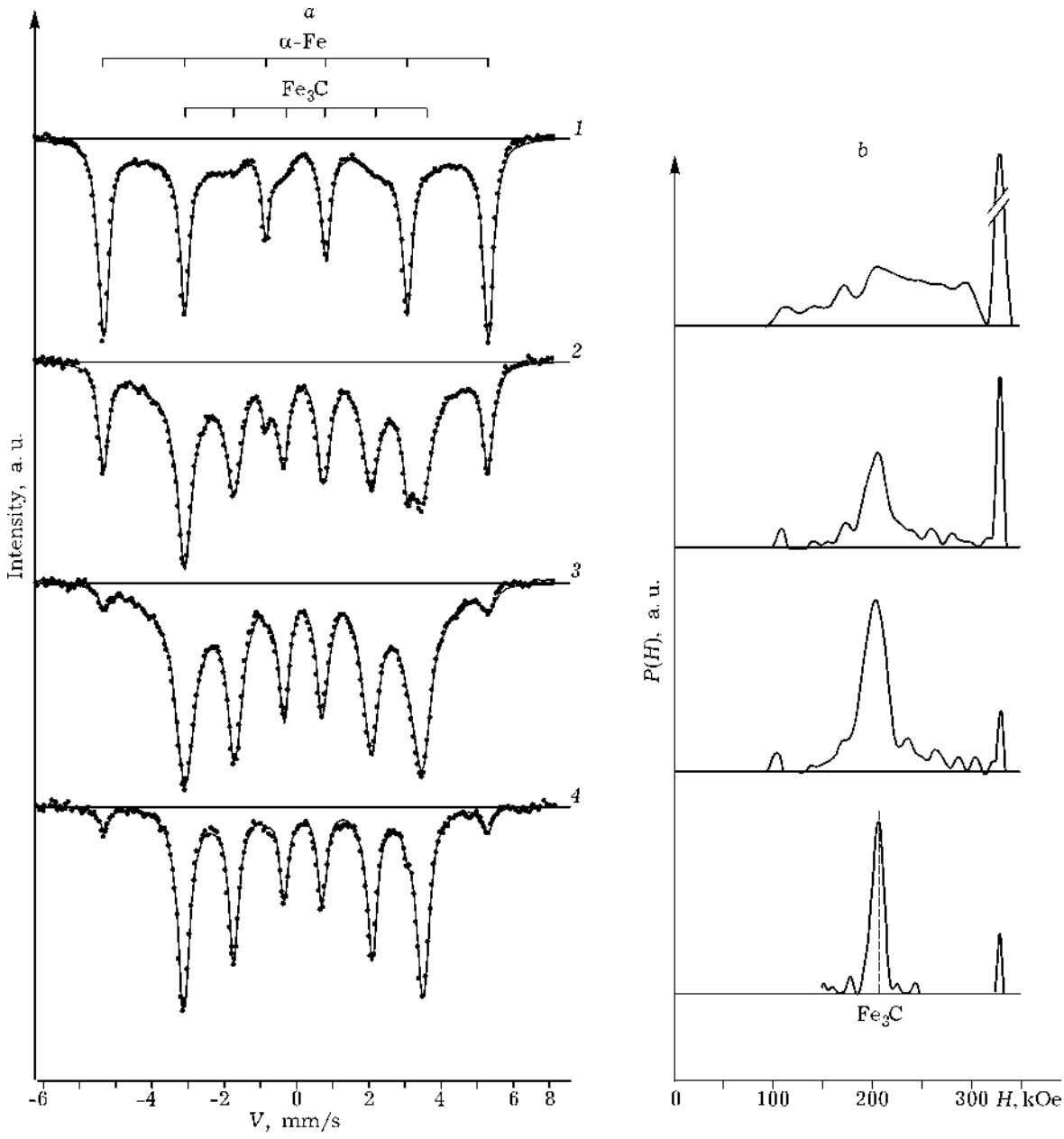

Fig. 6. Mössbauer spectra (*a*) and *P(H)* functions (*b*) of MA products in Fe(75)C(25) system. t_{mil}, h: 2 (*1*), 4 (*2*), 16 (*3*), and 16 + 1 (500 °C) (*4*).

with respect to the non-resonance level (it is shown by a horizontal line) and the availability of the broad distribution of HFMF from 100 to 300 kOe (see Fig. 6, *b*) in the *P*(*H*) function, respectively, one can draw the conclusion about the beginning of mechanical alloying of the Fe and C powders. In C(*T*) dependences (see Fig. 7) for t_{mil} = 1 and 2 h a bend is found at T = 570–580 K (shown by an arrow), which does not correspond to the Curie temperature of carbides. It follows from the results presented that at the initial stage of MA the amorphous Fe – C phase is formed. The average value of the HFMF of this phase is 225 kOe, which corresponds, according to [10], to the C concentration of 25 at. %.

With t_{mil} increasing, X-ray diffraction patters exhibit the new broadened peaks, whose positions correspond to the Fe_3C carbide (cementite). At t_{mil} = 16 h the contribution from the new system of peaks becomes predominant. In the MS (see Fig. 6) an additional sextet with

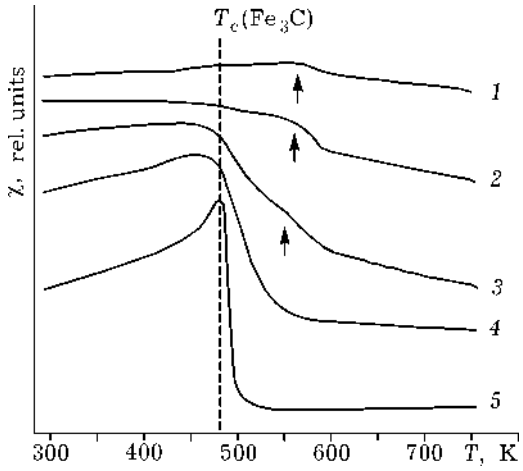

Fig. 7. Temperature dependences of a. c. magnetic susceptibility of Fe(75)C(25) powders. t_{mil}, h: 1 (*1*), 2 (*2*), 4 (*3*), 16 (*4*), and 16 + 1 (500 °C) (*5*).

the hyperfine parameters (H = 209 kOe, δ = 0.2 mm/s with respect to α-Fe and Δ = 0.1 mm/s) of cementite appears. The maximum intensity of the new component in the MS is also achieved at t_{mil} = 16 h. The results obtained are confirmed by the σ(T) temperature dependences (see Fig. 7). A vertical dashed line shows the Curie temperature of the Fe_3C carbide. To prove the formation of cementite, possibly with a distorted structure, after 16 h of milling the sample was annealed at T = 773 K for 1 h. The data given in Figs. 5, 6 and 7 unequivocally demonstrate the availability of a non-distorted Fe_3C carbide in the annealed sample.

Thus, from the results presented, it follows that in the MA of Fe with *sp*-elements having a much smaller covalent radius (C) compared to Fe, the sequence of solid-state reactions changes (amorphous Fe – C phase ® Fe_3C carbide). The data on partial amorphization of samples at the initial stage of MA and the following formation of cementite agree with the results of [11].

The results of the quantitative analysis of the MA process in the Fe(75)C(25), Fe(75)Si(25) and Fe(68)C(32) mixtures are given in Fig. 8. One can see that the time dependence of the amorphous phase Fe – C and ε-FeSi content is the same except for the twice as much difference in their maximal amount at t_{mil} = 2 h. Nevertheless, considering the time dependences of the phase content which appear at the second stage of MA, *i. e.* Fe_3C and α-Fe(Si) (see Fig. 8, *b*), one can draw the conclusion on the α-Fe(Si) SSS formation at shorter times of milling compared to cementite. Moreover, the comparison of the dependences of the phases content in MA of the Fe(68)Si(32) (see Fig. 3) and Fe(75)Si(25) (see Fig. 8) mixtures shows that the decrease of the Si concentration in the initial mixture results in the increase of the SSR rate. As well as for the Fe(68)M(32): M = Si, Ge, Sn mixtures we arrive at the conclusion that SSR in MA of Fe(75)C(25) and Fe(75)Si(25) proceed under the condition of realization of a nanostructure state in the α-Fe particles (see Fig. 8, *c*). The peculiarity of the Fe – C system is that increasing C concentration in the initial mixture to 32 at. % leads to transformation of cementite into a high-carbon Fe_7C_3 carbide (see Fig. 8, *d*).

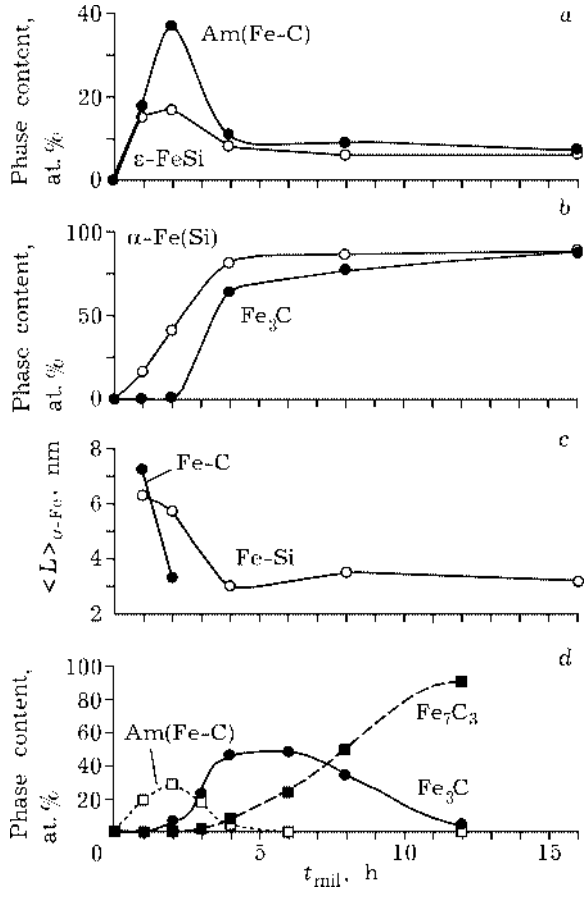

Fig. 8. Phase amounts (*a*, *b*), α-Fe grain sizes (*c*) in Fe(75)C(25) and Fe(75)Si(25) systems and phase amount in Fe(68)C(32) system (*d*) as a function of milling time.

A microscopic model of mechanical alloying in the Fe – M (M = C, Si, Ge, Sn) systems

The results presented illustrate that under the given conditions of milling t_{mil} =1 h is sufficient for a-Fe to reach a nanocrystalline state $<L> \leq 10$ nm. To account for the experimental data on MA, we refer to the considerations on the interface regions involving the boundary and close-to-boundary distorted zones. According to [12] the boundary width is one interplane distance, there being zones with a distorted structure along both sides of the boundary. In [13, 14] we estimated the width (d) of the interface region to be equal to ~1 nm. From Figs. 3 and 8 one can see that the maximum amount of the phases formed at the 1st stage (intermetallic compounds or amorphous Fe – C structure) corresponds to the grain sizes $<L>$ = 12, 6 and 3 nm. With d = 1 nm the volume fraction P_v of interfaces is 12, 23 and 43 %, respectively. From the comparison with the experimental data, we come to the conclusion that the 1st stage of MA is due to *sp*-atoms penetration along the grain boundaries and formation of either intermetallic phases (for the atoms having equal or larger radius compared to that of Fe) or amorphous phase (the atom of a small radius) in the interface regions. The exception is the Fe – Sn system. According to $<L>$ = 12 nm, we should have obtained the $FeSn_2$ amount @10–15 % which is actually 3 times as little as the observed experimental value of 37 % (see Fig. 3, *a*). This difference, in our opinion, is due to the low melting temperature of Sn (232 °C). The heating of the sample to 60 °C in milling and local increase of temperature on ΔT = 100–150 °C [2] at the expense of the heat released in the $FeSn_2$ formation can result in a pure Sn fusion and a considerable growth of $FeSn_2$ not only in the interface regions but in the contact places of Sn and Fe particles. As a proof of the *sp*-element penetration along a-Fe grain boundaries at early stages of MA, we present the X-ray diffraction data of pure components Fe, Sn and Ge fraction as a function of milling time (Fig. 9). Apparent increase of the a-Fe content and decrease of the Sn and Ge contents for t_{mil} < 1 h, while new phases have not be formed, testifies to that Sn and Ge are transferred into Fe grain boundary. On reaching $<L> \leq 3$ nm the existence of intermetallic phase becomes energetically unfavorable in the Fe – M (M = Si, Ge, Sn) systems; they decompose forming supersaturated solid solutions.

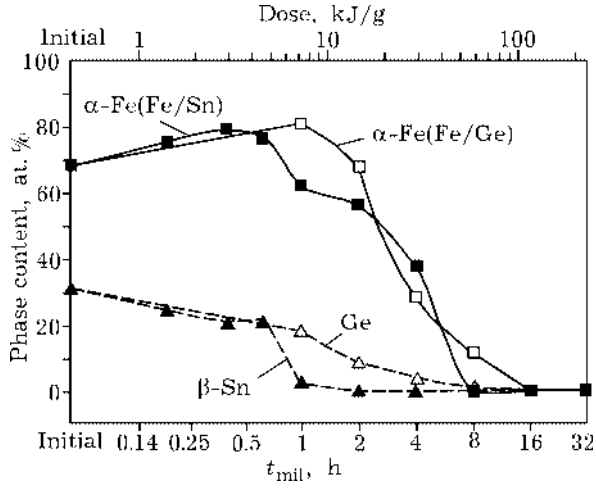

Fig. 9. Time dependences of pure components fraction during MA in Fe(68)Sn(32) and Fe(68)Ge(32) systems according to X-ray diffraction data.

Concerning saturation of solid solutions by Si, Ge and Sn one can make the following supposition. At present, two possible mechanisms of accelerated diffusion in MA are discussed. There are interstitial diffusion at the moment of collision [15] and diffusion along dislocations [16]. Taking into account the ratio of the component sizes in the Fe – Si and Fe – Sn systems, one can suppose that the accelerated diffusion in the Fe – Si system is mainly carried out along interstitials, but in the Fe – Sn system, dislocation transfer is carried out. Since the density of interstitials is always higher than of dislocations, the saturation rate of the solid solution in the Fe – Si system should be higher than in the Fe – Sn system. However, it is known [17] that with the grain size of $<L>$ < 10 nm there are no dislocations in the grain bulk. We consider the dislocation transfer as the nucleation of dislocation at the moment of impact, its passing through the grain body and leaving for the boundary. Such a process can provide the delivery of the second component (Sn) into the grain bulk of a-Fe. A different case is realized in the Fe – C system. Carbon has very low solubility in non-distorted *bcc* structure of a-Fe (<0.0001 % at 473 K). Thus, at the expense of the interstitial diffu-

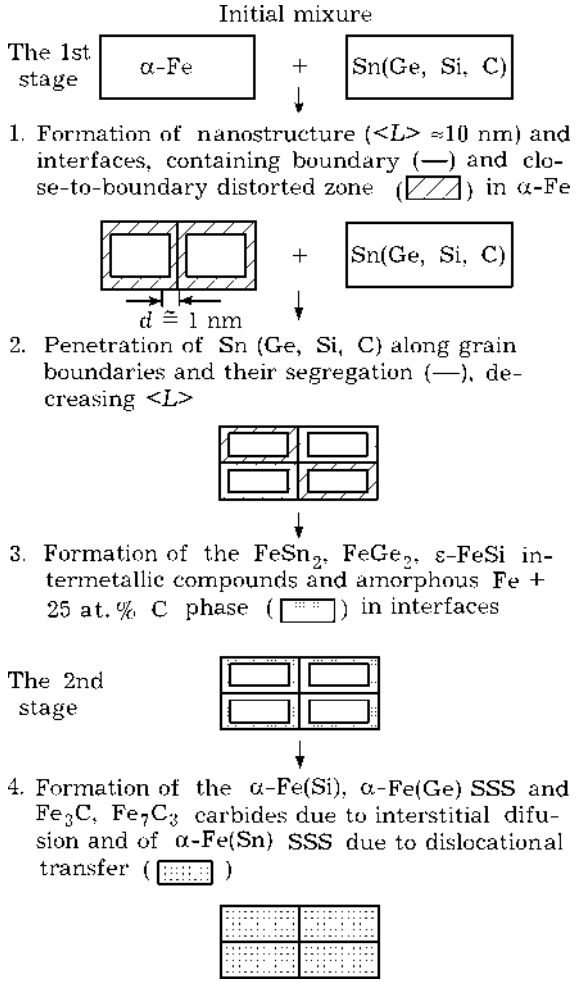

Fig. 10. Scheme of deformation atomic mixing during MA in Fe – M systems.

sion it can penetrate from the grain boundaries only into the close-to-boundary distorted zone, the amorphous Fe – C phase being formed with 25 at. % C. As the fraction of interface regions reaches its maximum value at t_{mil} = 2 h ($<L>_{a\text{-}Fe}$ = 3 nm), the amount of C in the amorphous phase is only 40 % out of the total amount of C in the initial mixture. The t_{mil} increase would have to lead to the C concentration increase in the amorphous phase. However, as it is illustrated by the experimental data, the formation of a distorted cementite in the interface regions is energetically favourable. At t_{mil} = 4 h (see Fig. 8) the sample consists of a-Fe + Fe_3C nanocomposite particles and particles of non-reacted carbon. At t_{mil} > 4 h carbon penetrating along new grain boundaries provides an increase of the cementite amount. However, the rate of cementite formation becomes much slower (see Fig. 8, *c*). If the amount of C in the initial mixture exceeds 25 at. % (the case of Fe(68)C(32)), then beginning with t_{mil} = 4 h the Fe_3C ® Fe_7C_3 transformation takes place. It is obvious that this reaction goes on at the moment of pulse effects and follows the mechanism of the interstitial diffusion between Fe_3C phase and C being in the interface.

The scheme of deformation atomic mixing during the MA process in Fe – M systems examined is presented in Fig. 10. There is no doubt that the suppositions on the accelerated mass transfer require further experimental and theoretical investigations to confirm or revise them.

CONCLUSIONS

1. Common regularities of MA in binary Fe–M (M = C, Si, Ge, Sn) mixtures are the formation of the nanocrystalline state in a-Fe at the initial stage and penetration of *sp*-elements along grain boundaries of a-Fe, the formation of the first Fe – M phase in the interface region (boundary and close-to-boundary distorted zone).

2. For the *sp*-elements with close and larger (compared to the Fe atom) radii (Si, Ge, Sn), the most stable intermetallic compounds (e-FeSi, $FeGe_2$, $FeSn_2$) are formed at the first stage; at the second one – supersaturated solid solutions. The ratio of the radii affects the kinetics of SSR. The experimental results are confirmed by thermodynamic calculations.

3. The *sp*-atom of a small radius (C) changes the sequence of solid state reactions in MA: amorphous Fe – C phase ® Fe_3C carbide for the Fe(75)C(25) mixture and amorphous Fe – C phase ® Fe_3C ® Fe_7C_3 for the Fe(68)C(32) mixture.

4. A microscopic model of MA based on the hypothesis concerning the interstitial and dislocation diffusion of *sp*-atoms at the moment of pulse mechanical effects is suggested.

Acknowledgements

This work is supported by the Russian Foundation for Basic Research (project 00–03–32555).

REFERENCES

1 E. P. Yelsukov, G. A. Dorofeev, V. A. Barinov *et al.*, *Mater. Sci. Forum*, 269–272 (1998) 151.
2 G. A. Dorofeev, G. N. Konygin, E. P. Yelsukov *et al.*, in M. Miglierini and D. Petridis (Eds.), Mössbauer Spectroscopy in Materials Science, Kluwer Acad. Publ., the Netherlands, 1999, p. 151.
4 G. A. Dorofeev, A. L. Ulyanov, G. N. Konygin and E. P. Yelsukov, *FMM*, 91 (2001) 44.
5 G. A. Dorofeev, E. P. Yelsukov, V. M. Fomin *et al.*, *Fizika i khimiya obrabotki materialov*, 2001 (in press).
6 E. P. Yelsukov, G. A. Dorofeev, G. N. Konygin *et al.*, *FMM*, 2001 (in press).
7 E. P. Yelsukov, G. A. Dorofeev, A. L. Ulyanov *et al.*, *Fizika i khimiya obrabotki materialov* (in press).
8 A. F. Cabrera, F. H. Sanchez and L. Mendoza-Zelis, *Mater. Sci. Forum*, 312–314 (1999) 85.
9 V. M. Fomin, E. V. Voronina, E. P. Yelsukov and A. N. Deev, *Ibid.*, 269–272 (1998) 437.
10 E. Bauer-Grosse and G. Le Caër, *Phil. Mag.*, B56 (1987) 485.
11 S. J. Campbell, G. M. Wang, A. Calka and W. A. Kaczmarek, *Mater. Sci. Eng.*, A226–228 (1997) 75.
12 Z. Horita, D. J. Smith, M. Furakawa *et al.*, *Mater. Characteriz.*, 37 (1996) 285.
13 E. P. Yelsukov, S. F. Lomaeva, G. N. Konygin *et al.*, *Nanostruct. Mater.*, 12 (1999) 483.
14 E. P. Yelsukov, G. A. Dorofeev, A. L. Ulyanov *et al.*, *FMM*, 91 (2001) 46.
15 P. Yu. Butyagin, *Chem. Rev.*, B23, Part 2 (1998) 89.
16 R. B. Schwarz, *Mat. Sci. Forum*, 269–272 (1998) 663.
17 M. L. Treudeau and R. Schulz, *Mater. Sci. Eng.*, A134 (1991) 1361.